Separation Science and Technology
Publication details, including instructions for authors and subscription information:
http://www.informaworld.com/smpp/title~content=t713708471

Quantitative Flux Analysis of Gas-Liquid Two-Phase Ultrafiltration

T. W. Cheng[a]; J. G. Wu[a]
[a] Department of Chemical Engineering, Tamkang University, Tamsui, Taipei, Taiwan

Online publication date: 20 February 2003

To cite this Article Cheng, T. W. and Wu, J. G.(2003) 'Quantitative Flux Analysis of Gas-Liquid Two-Phase Ultrafiltration', Separation Science and Technology, 38: 4, 817 — 835
To link to this Article: DOI: 10.1081/SS-120017628
URL: http://dx.doi.org/10.1081/SS-120017628

MARCEL DEKKER, INC. • 270 MADISON AVENUE • NEW YORK, NY 10016

SEPARATION SCIENCE AND TECHNOLOGY
Vol. 38, No. 4, pp. 817–835, 2003

Quantitative Flux Analysis of Gas–Liquid Two-Phase Ultrafiltration

T. W. Cheng* and J. G. Wu

Department of Chemical Engineering, Tamkang University, Tamsui, Taipei, Taiwan

ABSTRACT

The gas–liquid two-phase upward-flow ultrafiltration in a hollow-fiber membrane module with dextran aqueous solution as tested solution is studied in this work. The permeate fluxes are measured under various feed concentrations, superficial liquid velocities, superficial gas velocities, and transmembrane pressures. The flux increases with the increase in liquid velocity, gas velocity, and the transmembrane pressure, and decreases with the increase in the feed concentration. The flux enhancement by gas slugs is particularly significant when the ultrafiltration system is operated at a lower liquid velocity. The resistance-in-series model combined with the modified gel polarization model is applied to obtain the mass transfer coefficient of the gas–liquid two-phase ultrafiltration, and the dimensional analysis technique is used to find the correlation equation of the mass transfer coefficient. Furthermore, the flux equation for

*Correspondence: T. W. Cheng, Department of Chemical Engineering, Tamkang University, Tamsui, Taipei 251, Taiwan; Fax: +886-2-26209887; E-mail: twcheng@mail.tku.edu.tw.

DOI: 10.1081/SS-120017628 0149-6395 (Print); 1520-5754 (Online)

gas-sparging ultrafiltration is proposed. The predicted fluxes agree well with the experimental data.

Key Words: Ultrafiltration; Gas–liquid two-phase flow; Mass transfer coefficient; Dimensional analysis; Flux equation.

INTRODUCTION

Membrane ultrafiltration of macromolecular solutions has become an increasingly important separation process. The applications of ultrafiltration process[1,2] include the treatment of industrial effluents, oil emulsion wastewater, colloidal paint suspensions, biological macromolecules, and medical therapeutics. Membrane ultrafiltration is a pressure-driven separation process, typically in the range of 100 to 1000 kPa. The applied pressure provides the driving potential to force the solvent or the small solute to permeate through the membrane, while the large solute is rejected by the membrane. The rejected solute accumulates near the membrane surface; this is known as the concentration polarization phenomenon. Meanwhile, the solutes may cause membrane fouling. Both concentration polarization and membrane fouling increase the filtration resistance and reduce the permeate flux. In the search of ways to decrease those phenomena in order to increase the permeate flux, the method of gas–liquid two-phase flow is known as a simple and economical technique in enhancing the permeate flux of membrane filtration.[3–11] This method not only offers stable and large permeate flux but also saves energy. The addition of air to the liquid stream increases turbulence on the membrane surface and suppresses the formation of the concentration boundary layer, leading to enhancing flux of the filtration process. Recent researches indicate that tilting the membrane could further enhance the flux of gas–liquid two-phase ultrafiltration.[12,13]

Bellara et al.[7] investigated the use of gas sparging to overcome the concentration polarization in the ultrafiltration of macromolecular solutions with pilot-plant scale hollow-fiber modules. Their work showed that the flux enhancements were 20–50% for dextran (MW 83,000) in the module containing 3,600 fibers with 30,000 MWCO and 10–60% for albumin (MW 66,000) in the module containing 480 fibers with 200,000 MWCO, and the sieving coefficient of albumin was considerably reduced as gas sparging was introduced. Experiment conducted in a laboratory scale hollow-fiber module (15 fibers with a mean pore diameter 0.01 μm) also showed that the flux enhancement was 60–110% by the injecting gas on the ultrafiltration of clay (mean particle diameter = 1 μm) suspensions.[9] Performance of gas

introduction between the above two studies is different. The effect of injecting gas on flux enhancement is mainly related to two factors, the two-phase flow pattern and the filtration resistance of polarization layer existing in the liquid-phase ultrafiltration. Mercier et al.[8] pointed that the slug flow pattern is the best regime in increasing the filtration flux. Cheng et al.[11] further indicated that a threshold of gas velocity is required to disturb the polarization layer existing in the liquid-phase ultrafiltration. Beyond the critical gas velocity, gas slugs largely enhance the permeate flux.

The two-phase flow pattern in capillary tube depends on the injection ratio, defined as $u_G/(u_G + u_L)$ where u_G and u_L are, respectively, the superficial gas and liquid velocities. Experimental observations on the flow pattern in capillaries of 1–4 mm inner diameter show that the flow pattern slug flow in the range of injection ratio varies between 0.17 and 0.67, and the liquid slug contained no small dispersed bubbles.[14] This type of flow pattern is also called elongated bubble flow. The transition from slug flow to annular flow is about 0.9 injection ratio. Observations in tubes of 2–8 mm inner diameter also indicated that the flow pattern was elongated bubble flow for injection ratio varying between 0.06 and 0.66.[15] Barnea et al.[16] indicated that the elongated bubble flow exists in the regime of $u_L < 1.0\,m/s$ and $u_G < 1.0\,m/s$ in a 4-mm-diameter vertical tube. Result of Barnea et al.[16] also implied that the regime of elongated bubble flow enlarges as the tube diameter changed from 12.3 mm to 4 mm. The injection ratios were 0.03–0.12 and 0.1–0.7, respectively, in works of Bellara et al.[7] and Cabassud et al.[9] In addition, the inner diameters of fibers used were less than 1 mm. The flow patterns of both works could be assessed as the elongated bubble flow. Therefore, the difference in flux enhancement by gas slugs between the studies of Bellara et al.[7] and Cabassud et al.[9] may mainly relate to the filtration resistance existing in the polarization layer of the liquid-phase ultrafiltration. When the filtration resistance of polarization layer is large, the flux enhancement will be significant if a required gas velocity is introduced. A high polarization layer resistance in liquid-phase ultrafiltration is resulted from low crossflow velocity, high transmembrane pressure, high feed concentration, or low diffusivity of solute.

The hydrodynamics of gas–liquid two-phase ultrafiltration are more complicated than that of the single liquid phase system. Some researches have dealt with modeling the flux of gas-sparged ultrafiltration. Ghosh and Cui[17] divided the region near the gas slug into three zones: falling film zone, wake zone, and liquid slug zone. The mass transfer coefficients of the three zones were determined based on hydrodynamics. Then, the permeate flux in each zone was calculated by using the concentration polarization equation together with osmotic pressure model. Finally, the averaged permeate flux was

estimated from the combination of local permeate flux with the zone length in the tubular membrane. The calculated procedure is pretty complex and the estimation of the length of wake zone is doubtful. Vera et al.[18,19] used two dimensionless numbers, the shear stress number and the resistance number, to show the influence of gas sparging on the flux of microfiltration or ultrafiltration. Abdel-Ghani[20] modified the Leveque's equation in order to estimate the mass transfer coefficient of gas–liquid two-phase ultrafiltration. However, the modified equation is empirical with lack of physical interpretation. Cabassud et al.[21] defined a pulsation Reynolds number for the slug flow to quantify fluid mixing or turbulence near the membrane surface. A linear relationship was established between the flux enhancement and the pulsation Reynolds number. One objective of this work is to evaluate the mass transfer coefficient of gas–liquid two-phase ultrafiltration and discuss the influences of operating parameters on the mass transfer coefficient. The method of dimensional analysis will be applied in order to obtain the correlation equation of mass transfer coefficient in a two-phase ultrafiltration. The method has been adopted to correlate the mass transfer coefficient of ultrafiltration in a rotating filtration device.[22] Furthermore, the flux equation for predicting the flux of gas–liquid two-phase ultrafiltration system will be proposed in this study.

EXPERIMENTAL

The experimental apparatus used in this work is shown in Fig. 1. This gas–liquid two-phase ultrafiltration experiment was conducted in a hollow-fiber membrane module (H1P30-20, Amicon Co.) with upward co-current flow. The membrane material is polysulfone with 30,000 Da MWCO, 0.153 cm length, and 0.06 m^2 effective membrane area (about 250 fibers with 0.5 mm diameter in the module). The tested solute was Dextran T500 (Pharmacia Co.) which is more than 99% retained by the membrane used. The solvent used was distilled water. After each experiment, the membrane was cleaned by a combination of high circulation and backflushing with distilled water. Pure water permeability experiments were carried out to assess the cleanliness of the membrane.

The feed solution was circulated by a high-pressure pump with a variable speed motor (L-07553-20, Cole-Parmer Co.). The liquid flow rate was observed by a flowmeter (IR-OPFLOW 502-111, Headland Co.). The compressed air supply was directed to the liquid stream with the rate of gas addition monitored by a flowmeter (F150-AV1-B-125-30-SAP, Porter Co.). The feed pressure was controlled by using an adjustable valve at the outlet of the membrane module,

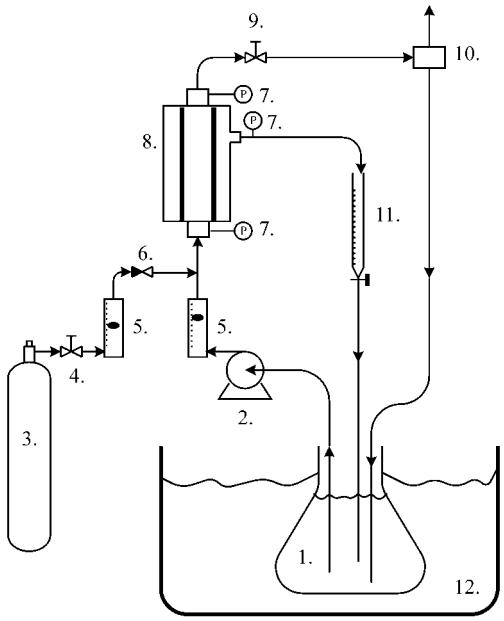

1. feed tank
2. pump
3. compressed air
4. air flow rate adjustment valve
5. flow meter
6. one-way valve
7. pressure gauge
8. membrane module
9. pressure control valve
10. gas/liquid separator
11. collector
12. thermostat

Figure 1. Flow diagram of gas–liquid two-phase ultrafiltration apparatus.

and the gauge pressures at the tubeside inlet (p_i), outlet (p_o), and at the shellside (p_p) were measured with a pressure transmitter (Model 891.14.425, Wika Co.). During operation, both the permeate and the retentate were recycled back to the feed tank for keeping the feed concentration constant.

The ranges of the experimental conditions were chosen as follows. The feed concentrations, c_i, were 2.0–16.0 g/l; the inlet transmembrane pressures, Δp, were 58.8–156.8 kPa; the liquid superficial velocity, u_L, were 0.10–0.30 m/s; and the gas superficial velocity, u_G, were 0.01–0.15 m/s. According to the liquid superficial velocity, the single liquid-phase flow is laminar, and the corresponding air injection ratio, i.e., $u_G/(u_G + u_L)$, ranges from 0.03 to 0.6. The feed solution temperature in all experiments was kept at 30°C by a thermostat.

RESULTS AND DISCUSSION

Flow Pattern and Flux Characteristics

Observations on the gas–liquid two-phase flow pattern in the small diameter tubes (i.d. 2–8 mm) showed that the flow pattern is elongated bubble in the range of $0.168\,\mathrm{m/s} < u_L < 0.672\,\mathrm{m/s}$ and $0.04\,\mathrm{m/s} < u_G < 0.32\,\mathrm{m/s}$.[15] Barnea et al.[16] indicated that the elongated bubble flow exists in the regime of $u_L < 1.0\,\mathrm{m/s}$ and $u_G < 1.0\,\mathrm{m/s}$ in a 4-mm-diameter vertical tube. Result of Barnea et al.[16] also implied that the regime of elongated bubble flow enlarges as the tube diameter changed from 12.3 mm to 4 mm. In this study, the liquid superficial velocity, u_L, were 0.10–0.30 m/s; and the gas superficial velocity, u_G, were 0.01–0.15 m/s. According to the results of the above works, the flow pattern of the present gas–liquid two-phase flow can be confirmed to be elongated bubble flow.

Figure 2 shows the effect of air sparging on filtration flux at a specified operating condition. When a small amount of gas ($u_G = 0.01\,\mathrm{m/s}$) was introduced into the conventional liquid-phase ultrafiltration, the permeate flux

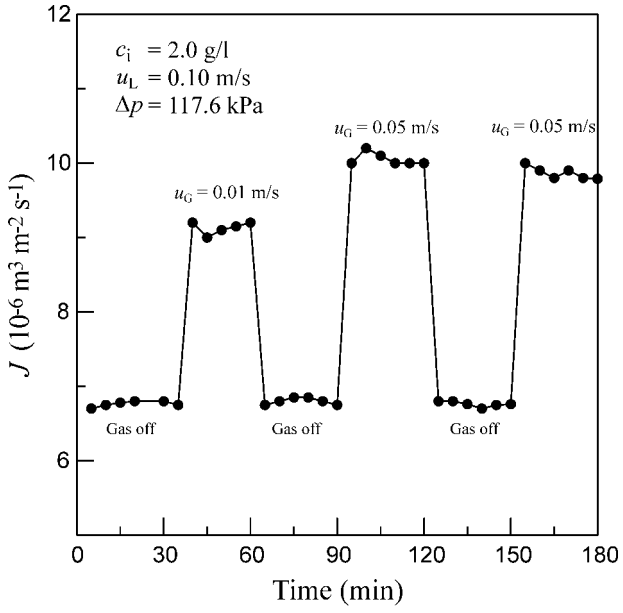

Figure 2. Flux characteristics under various gas velocities.

increased and the flux enhancement was about 35%. The permeate flux restored to the liquid-phase ultrafiltration flux immediately as the gas supply was turned off. When gas introduction was turned on to $u_G = 0.05\,m/s$, the flux was enhanced up to 50%. The experiment result shows that the ultrafiltration system has a good reproduction on flux presentation. The addition of air into the conventional liquid-phase ultrafiltration can increase turbulence on the membrane surface and suppress the formation of the concentration layer, leading to an increase in the permeate flux. A steady flux can be reached within 30 minutes after changing the gas flow rate.

Flux Enhancement Under Various Gas Velocities

Figure 3 shows the permeate flux vs. transmembrane pressure under various gas velocities in the condition of 8.0 g/l feed concentration and 0.1 m/s superficial liquid velocity. The permeate flux increases as the transmembrane pressure increases in the pressure range examined. However, the permeate flux tends to approach a limiting flux if the transmembrane pressure further increases. It is noted that the addition of gas slugs into the liquid stream can

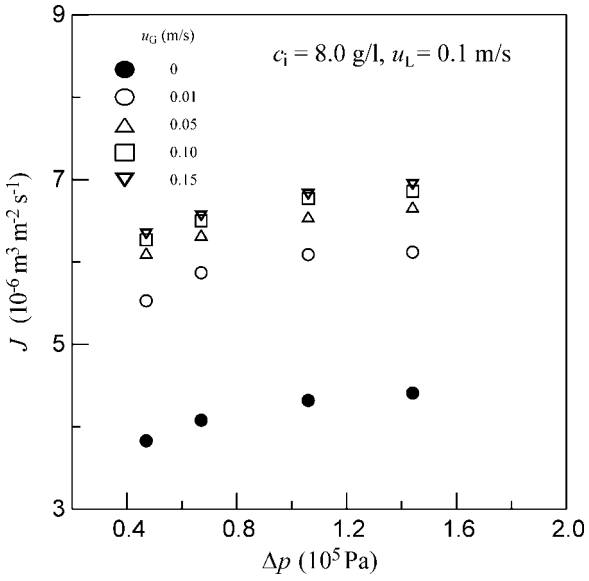

Figure 3. Flux vs. transmembrane pressure for different gas velocities.

enhance the flux significantly. The effect of gas slugs on the flux enhancement depends on the extent of concentration polarization in the single liquid-phase ultrafiltration operation; a threshold of gas velocity is required to disturb the concentration polarization layer.[11] In the present condition, the addition of an amount of 0.01 m/s gas flow is enough to enhance the flux up to about 40%. The flux enhancement reaches 60% when the gas velocity increases to 0.1 m/s. The flux enhancement increases initially with the increase in the gas velocity and then approaches a limit as the gas velocity further increases.

Limiting Flux and Gel Layer Concentration

Ultrafiltration is a pressure-driven separation process; the permeate flux of ultrafiltration is usually proportional to the transmembrane pressure at a small applied pressure. However, owing to the formation of a high solute concentration or a gel layer on the membrane surface, the flux will approach a limiting flux as the transmembrane pressure further increases. The limiting flux can be obtained from the experimental data at a sufficiently high pressure or be determined by applying the resistance-in-series model.[23]

The resistance-in-series model was used to determine the limiting permeate flux in this work. The procedure is shown as follows. At a specific flow velocity and feed concentration, the permeate flux can be expressed as

$$J = \frac{\Delta p}{R_m + R_f + R_p} \tag{1}$$

where R_m is the intrinsic membrane resistance, R_f is the resistance caused by membrane fouling due to membrane blockage and/or solute–membrane adsorption, and R_p represents the resistance caused by concentration polarization due to the build up of a concentration boundary layer near the membrane surface. In general, R_p is proportional to the applied pressure and is expressed as $\phi\Delta p$. From Eq. (1), when transmembrane pressure (Δp) is sufficiently large, the flux reaches the limiting flux (J_{lim}), thus ϕ is equal to $1/J_{lim}$. Equation 1 can be rearranged into

$$\frac{1}{J} = \frac{1}{J_{lim}} + \frac{R_m + R_f}{\Delta p} \tag{2}$$

From the experimental flux data of ultrafiltration, a least-square line could be determined from the plot of $1/J$ vs. $1/\Delta p$. The limiting flux (J_{lim}) as well as ($R_m + R_f$) can be determined from the intercept and the slope of the straight line.

Table 1 is the list of the determined J_{lim} and $R_m + R_f$ of the experiments under various feed concentrations, liquid velocities, and gas velocities. Experimental result shows that the limiting flux increases with increasing liquid or gas velocity, or decreasing feed concentration. Under high transmembrane pressure, the ultrafiltration flux is mass transfer controlled region. Therefore, increasing the mass transfer coefficient by increasing crossflow velocity or decreasing feed concentration is beneficial to heighten the flux.

As the limiting flux is reached, the concentration of the solute accumulated on the membrane surface is called gel layer concentration, c_g. The modified gel-polarization model[23] indicates that

$$J_{lim} = \bar{k} \ln \frac{c_g}{c_i} = F k_i \ln \frac{c_g}{c_i} \tag{3}$$

where $\bar{k}$ is the average mass transfer coefficient within the concentration polarization layer, F is a modified factor, and k_i is the mass transfer coefficient estimated with Leveque equation under the inlet feed condition as

$$k_i = 1.62 \left(\frac{u_i D_i^2}{2 r_m L} \right)^{1/3} \tag{4}$$

According to Eq. (3), a straight line can be obtained from the plot of experimental data, J_{lim}/k_i vs. $\ln c_i$, by the method of least squares. Value of c_g could be determined from the intersection on the concentration axis.

Figure 4 is the plot of J_{lim}/k_i vs. $\ln c_i$ of the present single liquid-phase ultrafiltration system. The gel layer concentration was about 76.7 g/l determined from Fig. 4. The concentration of gel layer could be applied to the gas–liquid two-phase ultrafiltration because the gel layer concentration is usually insensitive to the crossflow rate.[23]

Mass Transfer Coefficient of Two-Phase Ultrafiltration

The limiting flux of two-phase ultrafiltration, determined from the experimental flux data by using the resistance-in-series model, is shown in Table 1. The gel layer concentration has also determined from the single liquid-phase ultrafiltration system. Thus, the mean mass transfer coefficient of two-phase ultrafiltration system can be obtained by applying the modified

Table 1. Filtration resistances and limiting fluxes under various operating parameters.

		$u_L = 0.10\,\mathrm{m\,s^{-1}}$		$u_L = 0.15\,\mathrm{m\,s^{-1}}$		$u_L = 0.20\,\mathrm{m\,s^{-1}}$		$u_L = 0.30\,\mathrm{m\,s^{-1}}$	
c_i ($\mathrm{g\,l^{-1}}$)	u_G ($\mathrm{m\,s^{-1}}$)	$(R_m + R_f)$ ($10^8\,\mathrm{Pa\,m^2\,s\,m^{-3}}$)	J_{lim} ($10^{-6}\,\mathrm{m^3\,m^{-2}\,s^{-1}}$)	$(R_m + R_f)$ ($10^8\,\mathrm{Pa\,m^2\,s\,m^{-3}}$)	J_{lim} ($10^{-6}\,\mathrm{m^3\,m^{-2}\,s^{-1}}$)	$(R_m + R_f)$ ($10^8\,\mathrm{Pa\,m^2\,s\,m^{-3}}$)	J_{lim} ($10^{-6}\,\mathrm{m^3\,m^{-2}\,s^{-1}}$)	$(R_m + R_f)$ ($10^8\,\mathrm{Pa\,m^2\,s\,m^{-3}}$)	J_{lim} ($10^{-6}\,\mathrm{m^3\,m^{-2}\,s^{-1}}$)
2.0	0	15.50	7.62	14.23	8.72	10.94	9.07	10.04	10.55
	0.01	8.49	9.99	10.48	10.18	8.18	10.60	9.07	11.24
	0.05	7.38	10.88	8.12	10.94	6.71	11.14	8.45	11.48
	0.10	6.70	11.05	8.24	11.32	6.48	11.36	7.67	11.78
	0.15	6.81	11.25	7.91	11.45	6.22	11.58	7.36	12.05
4.0	0	16.78	6.02	14.01	6.84	11.77	7.12	8.86	8.37
	0.01	10.14	8.34	8.02	8.59	8.19	8.95	6.54	9.33
	0.05	7.73	8.97	5.87	9.33	5.97	9.34	4.94	9.47
	0.10	8.00	9.29	5.69	9.53	5.85	9.59	5.11	9.82
	0.15	7.45	9.34	5.95	9.66	5.34	9.67	5.04	10.04
8.0	0	24.22	4.78	21.03	5.39	18.36	5.99	14.83	6.80
	0.01	12.57	6.53	13.32	6.78	14.28	7.15	13.74	7.75
	0.05	9.61	6.97	9.68	7.32	12.71	7.57	12.39	7.88
	0.10	9.83	7.20	9.86	7.49	12.16	7.69	11.16	8.04
	0.15	9.74	7.28	10.27	7.62	10.76	7.65	11.18	8.29
16.0	0	29.81	3.89	29.19	4.45	24.23	4.80	24.18	5.50
	0.01	13.31	5.06	15.83	5.31	18.13	5.58	20.10	6.17
	0.05	12.24	5.53	13.22	5.83	15.93	5.92	19.40	6.28
	0.10	13.07	5.66	13.79	6.00	15.48	6.02	20.76	6.52
	0.15	13.35	5.70	14.81	6.10	15.70	6.13	20.01	6.61

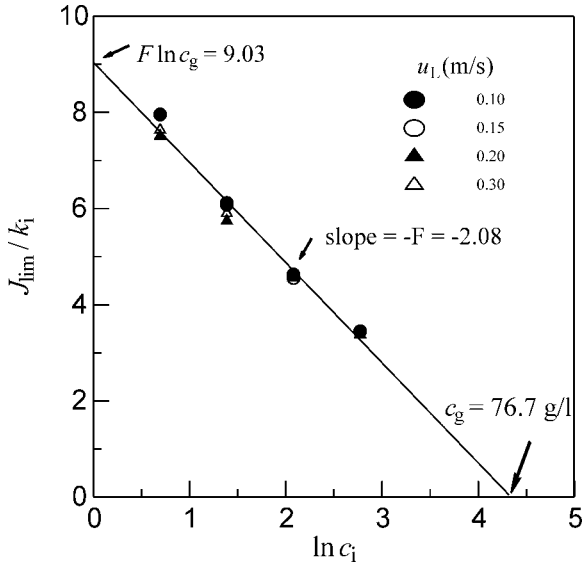

Figure 4. Limiting flux vs. feed concentration.

gel-polarization model

$$\bar{k} = \frac{J_{\lim}}{\ln(c_g/c_i)} \tag{5}$$

Table 2 is the list of the mass transfer coefficients calculated with Eq. (5) and under various operating conditions. The calculated results show that mass transfer coefficient increases with the increase in the gas velocity, liquid velocity, as well as the feed concentration.

After obtaining the mass transfer coefficients, the method of dimensional analysis was used to correlate the mass transfer coefficient in terms of operation parameters and physical properties. The mass transfer coefficient $\bar{k}$ is a function of the diameter of fiber d, the kinematic viscosity ν, diffusivity D, superficial gas velocity u_G, and superficial liquid velocity u_L. The relation of the parameters is assumed as the following form:

$$\mathrm{Sh} = A\mathrm{Re}_L^a \mathrm{Sc}^b (1 + u_G/u_L)^c \tag{6}$$

where $\mathrm{Sh} = \bar{k}d/D$ (Sherwood number), $\mathrm{Re}_L = u_L d/\nu$ (liquid Reynolds number), and $\mathrm{Sc} = \nu/D$ (Schmidt number). The constants A, a, b, and c are determined constants.

Table 2. Mass transfer coefficients of gas–liquid two-phase ultrafiltration.

c_i (g l^{-1})	u_G (m s^{-1})	$u_L = 0.10$ m s^{-1} $\bar{k}$ (10^{-6} m s^{-1})	$u_L = 0.15$ m s^{-1} $\bar{k}$ (10^{-6} m s^{-1})	$u_L = 0.20$ m s^{-1} $\bar{k}$ (10^{-6} m s^{-1})	$u_L = 0.30$ m s^{-1} $\bar{k}$ (10^{-6} m s^{-1})
2.0	0.01	2.74	2.79	2.91	3.08
	0.05	2.98	3.00	3.05	3.15
	0.10	3.03	3.10	3.11	3.23
	0.15	3.08	3.14	3.17	3.30
4.0	0.01	2.82	2.91	3.03	3.16
	0.05	3.04	3.16	3.16	3.21
	0.10	3.14	3.23	3.25	3.32
	0.15	3.16	3.27	3.27	3.40
8.0	0.01	2.89	3.00	3.16	3.43
	0.05	3.08	3.24	3.35	3.49
	0.10	3.19	3.32	3.40	3.55
	0.15	3.22	3.37	3.39	3.67
16.0	0.01	3.23	3.39	3.56	3.93
	0.05	3.53	3.72	3.78	4.00
	0.10	3.61	3.83	3.84	4.16
	0.15	3.64	3.89	3.91	4.21

The kinematic viscosity ν of Dextran T500 solution and the solute diffusivity D can be estimated from the following equations[23]

$$\nu = 0.89 \times 10^{-6} \exp(0.0371 c_{\mathrm{i}})\ \mathrm{m^2\ s^{-1}} \tag{7}$$

and

$$D \times 10^{11} = 1.20 + 2.61 \times 10^{-2} c_{\mathrm{i}} - 4.17 \times 10^{-5} c_i^2 + 2.13 \times 10^{-8} c_i^3\ \mathrm{m^2\ s^{-1}} \tag{8}$$

The unit of concentration in Eqs. (7) and (8) is g/l.

The values of constants A, a, b, and c can be determined from correlating the experimental data of Sh with the operating parameters. Using a heat–mass transfer analogy, the exponent b of the Schmidt number can be assumed to be 0.33.[22] The exponent a was determined by varying the liquid velocity under constant $u_{\mathrm{G}}/u_{\mathrm{L}}$. Then, the exponent c and constant A were obtained through variation of the ratio $u_{\mathrm{G}}/u_{\mathrm{L}}$, shown in Fig. 5. Finally, the correlation equation of mass transfer coefficient was obtained as

$$\mathrm{Sh} = 1.54 \mathrm{Re}_{\mathrm{L}}^{0.13} \mathrm{Sc}^{0.33} (1 + u_{\mathrm{G}}/u_{\mathrm{L}})^{0.17} \tag{9}$$

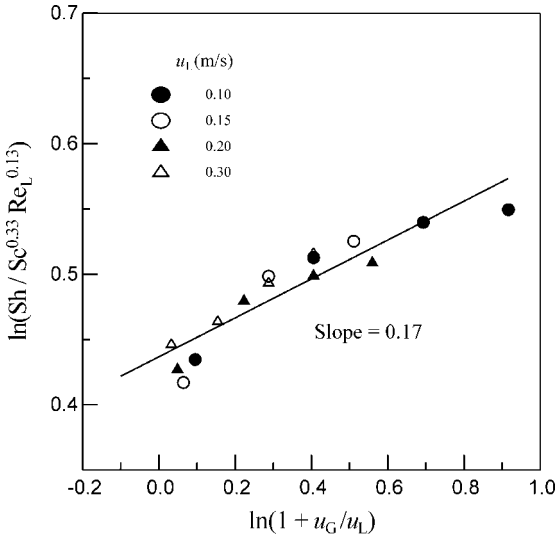

Figure 5. Correlation of mass transfer coefficient with operating parameters.

Flux Equation of Two-Phase Ultrafiltration

Combination of Eqs. (1) and (5), the flux equation for estimating the flux in the gas–liquid two-phase ultrafiltration can be expressed as

$$J = \frac{\Delta p}{R_m + R_f + [\Delta p/\bar{k}\ln(c_g/c_i)]} \tag{10}$$

in which the mass transfer coefficient is expressed in Eq. (9). Figure 6 is the plots of the calculated and experimental fluxes under the condition of 2.0 g/l feed concentration and 0.1 m/s liquid velocity. The predicted flux agrees well with the experimental data. The flux enhancement is about 150% when the gas velocity increases to 0.1 m/s. Figure 7 is the plot of the flux at a higher liquid velocity ($u_L = 0.3\,m/s$). The predicted flux agrees with the experimental data with a slight underestimation. Experimental result shows that the flux enhancement is less significant at a higher liquid velocity due to a less filtration resistance in liquid-phase ultrafiltration. The flux enhancement is about 110% at 0.1 m/s gas velocity in the case of $u_L = 0.3\,m/s$. Figure 8 is the plot of ultrafiltration flux under the condition of 0.3 m/s liquid velocity and 16.0 g/l feed concentration. The concentration polarization phenomenon is

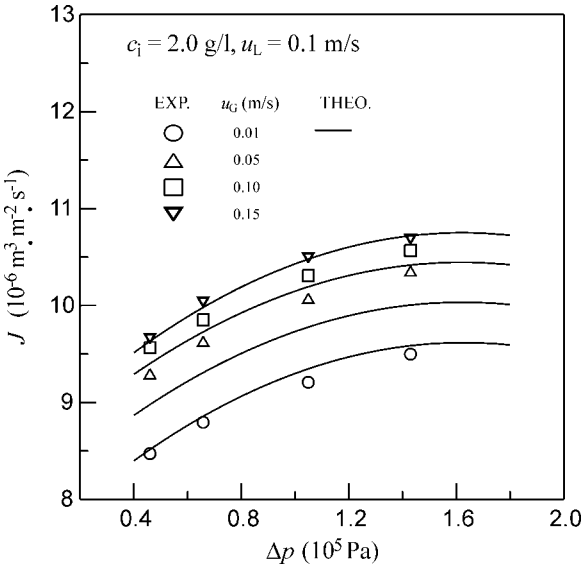

Figure 6. Predicted and experimental fluxes: $c_i = 2.0\,g/l$, $u_L = 0.1\,m/s$.

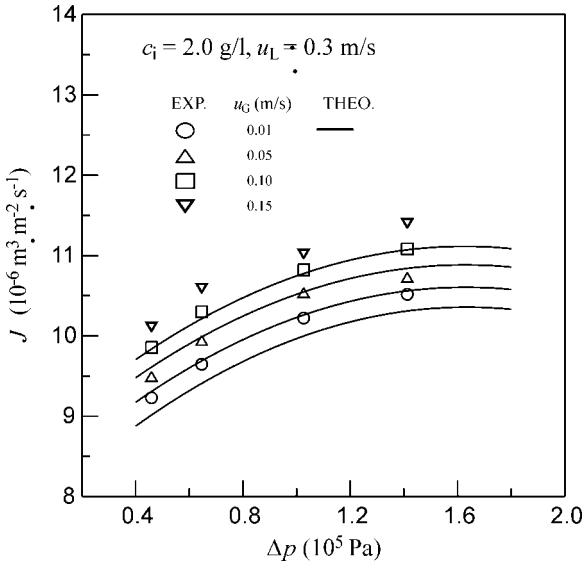

Figure 7. Predicted and experimental fluxes: $c_i = 2.0\,g/l$, $u_L = 0.3\,m/s$.

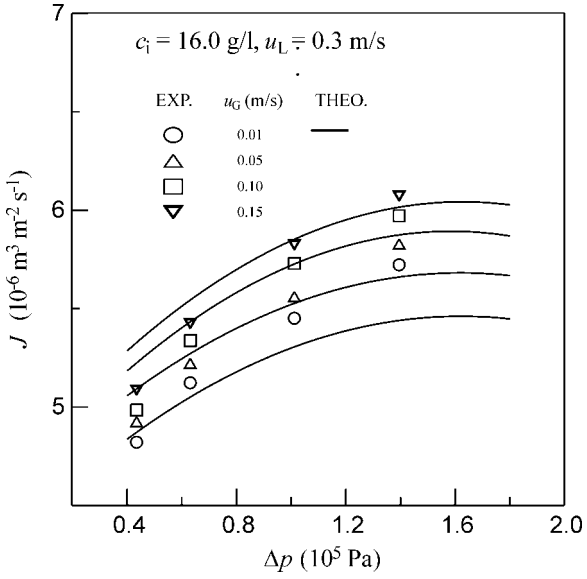

Figure 8. Predicted and experimental fluxes: $c_i = 16.0\,g/l$, $u_L = 0.3\,m/s$.

severe for operating at a high feed concentration. Though the flux of this case is lower, the flux enhancement by gas slugs is higher than that shown in Fig. 7. In general, the predicted flux calculated from the present equation is in a good trend with the experimental data. Average errors between the predictions and experimental data are defined as follows,

$$\varepsilon = \frac{\sum_{n=1}^{n=N} |J_{\text{pre},n} - J_{\text{exp},n}|/J_{\text{exp},n}}{N} \tag{11}$$

where N is the number of the experimental data, are less than 5%.

CONCLUSIONS

The gas–liquid two-phase crossflow ultrafiltration in the hollow-fiber membrane module was investigated with Dextran aqueous solution as tested solution. The flux increases with increasing the liquid superficial velocity, gas superficial velocity, and the transmembrane pressure whereas it decreases with the increase in the feed concentration. The maximum flux enhancement by gas slugs reaches 160% in this work. A method for evaluating the mass transfer coefficient of two-phase ultrafiltration was proposed and the dimensional analysis method was used to obtain the correlation equation of the mass transfer coefficient. The flux equation of the flux of gas–liquid two-phase ultrafiltration was developed based on the mass transfer equation and the resistance-in-series model. The predicted fluxes agree well with the experimental data in a wide range of operating conditions.

SYMBOLS

A	the determined constant in Eq. (6)
a	the determined constant in Eq. (6)
b	the determined constant in Eq. (6)
c	the determined constant in Eq. (6)
c_g	gel concentration (g/l)
c_{i}	feed concentration (g/l)
d	diameter of hollow fiber (m)
F	modified factor
J	permeate flux (m/s)
J_{lim}	limiting permeate flux (m/s)
k_{i}	mass transfer coefficient (m/s)

L	length of hollow fiber (m)
Δp	transmembrane pressure (Pa)
R_f	fouling resistance (Pa-s/m)
R_m	membrane resistance (Pa-s/m)
Re_L	liquid Reynolds number
Sc	Schmidt number
Sh	Sherwood number
u_G	superficial gas velocity (m/s)
u_L	superficial liquid velocity (m/s)
ε	average error
ν	kinematic viscosity (m^2/s)

ACKNOWLEDGMENT

The authors wish to express their thanks to the Nation Science Council of Taiwan ROC for financial aid.

REFERENCES

1. Porter, M.C. Membrane filtration. In *Handbook of Separation Techniques for Chemical Engineers*; Schweizter, P.A., Ed.; McGraw-Hill: New York, 1979; Section 2.1.
2. Kulkarni, S.S.; Funk, E.W.; Li, N.N. Ultrafiltration: applications and economics. In *Membrane Handbook*; Ho, W.S.W., Sirkar, K.K., Eds.; Van Nostrand Reinhold: New York, 1992; 446–453.
3. Imasaka, T.; So, H.; Matsushita, K.; Furukawa, T.; Kanekuni, N. Application of gas–liquid two-phase cross-flow filtration to pilot-scale methane fermentation. Drying Technol. **1993**, *11* (4), 769–785.
4. Lee, C.K.; Chang, W.G.; Ju, Y.H. Air slugs entrapped cross-flow filtration of bacterial suspensions. Biotechnol. Bioeng. **1993**, *41*, 525–530.
5. Cui, Z.F.; Wright, K.I.T. Gas–liquid two-phase cross-flow ultrafiltration of BSA and dextran solution. J. Membr. Sci. **1994**, *90*, 183–189.
6. Cui, Z.F.; Wright, K.I.T. Flux enhancements with gas sparging in downwards crossflow ultrafiltration: performance and mechanism. J. Membr. Sci. **1996**, *117*, 109–116.
7. Bellara, S.R.; Cui, Z.F.; Pepper, D.S. Gas sparging to enhance permeate flux in ultrafiltration using hollow fibre membranes. J. Membr. Sci. **1996**, *121*, 175–184.

8. Mercier, M.; Fonade, C.; Lafforgue-Delorme, C. Influence of the flow regime on the efficiency of a gas–liquid two-phase medium filtration. Biotechnol. Tech. **1995**, *9*, 853–858.
9. Cabassud, C.; Laborie, S.; Laine, J.M. How slug flow can improve ultrafiltration flux in organic hollow fibers. J. Membr. Sci. **1997**, *128*, 93–101.
10. Mercier, M.; Fonade, C.; Lafforgue-Delorme, C. How slug flow can enhance the ultrafiltration flux in mineral tubular membranes. J. Membr. Sci. **1997**, *128*, 103–113.
11. Cheng, T.W.; Yeh, H.M.; Gau, C.T. Enhancement of permeate flux by gas slugs for crossflow ultrafiltration in tubular membrane module. Sep. Sci. Technol. **1998**, *33* (15), 2295–2309.
12. Cheng, T.W.; Yeh, H.M.; Wu, J.S. Effects of gas slugs and inclination angle on the ultrafiltration flux in tubular membrane module. J. Membr. Sci. **1999**, *158*, 223–234.
13. Cheng, T.W. Influence of inclination on gas sparged cross-flow ultrafiltration through an inorganic tubular membrane. J. Membr. Sci. **2002**, *196*, 103–110.
14. Laborie, S.; Cabassud, C.; Durand-Bourlier, L.; Laine, J.M. Characterisation of gas–liquid two-phase flow inside capillaries. Chem. Eng. Sci. **1999**, *54*, 5723–5735.
15. Cheng, T.W.; Lin, T.L. Characteristics of gas–liquid two-phase flow in small diameter inclined tubes. Chem. Eng. Sci. **2001**, *56*, 6393–6398.
16. Barnea, D.; Luninski, Y.; Taitel, Y. Flow pattern in horizontal and vertical two phase flow in small diameter pipes. Can. J. Chem. Eng. **1983**, *61*, 617–620.
17. Ghosh, R.; Cui, Z.F. Mass transfer in gas-sparged ultrafiltration: upward slug flow in tubular membranes. J. Membr. Sci. **1999**, *162*, 91–102.
18. Vera, L.; Villarroel, R.; Delgado, S.; Elmaleh, S. Enhancing microfiltration through an inorganic tubular membrane by gas sparging. J. Membr. Sci. **2000**, *165*, 47–57.
19. Vera, L.; Delgado, S.; Elmaleh, S. Dimensionless numbers for the steady-state flux of cross-flow microfiltration and ultrafiltration with gas sparging. Chem. Eng. Sci. **2000**, *55*, 3419–3428.
20. Abdel-Ghani, M.S. Cross-flow ultrafiltration of an aqueous polymer foam solution produced by gas sparging. J. Membr. Sci. **2000**, *171*, 105–117.
21. Cabassud, C.; Laborie, S.; Durand-Bourlier, L.; Laine, J.M. Air sparging in ultrafiltration hollow fibers: relationship between flux enhancement, cake characteristics and hydrodynamic parameters. J. Membr. Sci. **2001**, *181*, 57–69.

22. Holeschovsky, U.B.; Cooney, C.L. Quantitative description of ultrafiltration in a rotating filtration device. AIChE J. **1991**, *37* (8), 1219–1226.
23. Cheng, T.W.; Yeh, H.M.; Gau, C.T. Resistance analyses for ultrafiltration in tubular membrane module. Sep. Sci. Technol. **1997**, *32* (16), 2623–2640.